Research Paper

MicroRNA-30b targets Snail to impede epithelial-mesenchymal transition in pancreatic cancer stem cells

Yicheng Xiong[1*], Yao Wang[2*], Lei Wang[2], Yan Huang[2, 3], Yang Xu[2, 3], Liancheng Xu[2, 3], Yibing Guo[3], Jingjing Lu[3], Xiaohong Li[3], Mingyan Zhu[2✉], Haixin Qian[1✉]

1. General Surgery Department, the First Affiliated Hospital of Soochow University, 215006, Suzhou, Jiangsu, P.R. China
2. General Surgery Department, Affiliated Hospital of Nantong University,226001, Nantong, Jiangsu, P.R. China
3. Clinical Medical Research Center, Affiliated Hospital of Nantong University, 226001, Nantong, Jiangsu, P.R. China

*These authors contributed equally to this work.

✉ Corresponding authors: E-mail: qianhaixin@suda.edu.cn (Haixin Qian); zmy5661@163.com (Mingyan Zhu)

Abstract

Snail-mediated epithelial-mesenchymal transition (EMT) process plays a fundamental role in facilitating pancreatic ductal adenocarcinoma (PDAC) stemness and metastasis. In the present study, we revealed that microRNA-30 (miR-30) members, especially miR-30b, were remarkably downregulated in triple-positive (CD24^{+}, CD44^{+}, EpCAM^{+}) pancreatic cancer stem cells (PCSCs). In addition, we revealed that miR-30b suppressed EMT process in PCSCs. Overexpression of miR-30b led to reduced expression of mesenchymal marker N-cadherin and the upregulation of epithelial marker E-cadherin. Moreover, both of TargetScan and PicTar algorithms predicted that miR-30b directly targeted Snail 3'UTR. Luciferase reporter assay showed that miR-30b could specifically reduce the translational activity of Snail wild-type 3'UTR, but not its mutant form. In line with these results, transwell assay demonstrated that overexpression of miR-30b mimic impaired migratory and invasive capacities of PCSCs. Furthermore, miR-30b overexpression suppresses in vivo tumorigenic potential of PDACs. Finally, a negative correlation between the expression of miR-30b and Snail was uncovered. Low level of miR-30b and high Snail expression both predict dismal prognosis in PDAC patients. Taken together, these findings implicate that miR-30b may suppress PCSC phenotype and PDAC metastasis through posttranscriptionally suppressing Snail expression, highlighting that miR-30b may serve as a therapeutic agent in the treatment of PDAC.

Key words: miR-30b; pancreatic ductal adenocarcinoma; pancreatic cancer stem cells; epithelial-mesenchymal transition; Snail

Introduction

Pancreatic ductal adenocarcinoma (PDAC) is one of the most lethal cancers, with an overall 5-year survival rate of approximate 5% [1]. Due to the lack of specific symptoms in early stages and the absence of effective screening approaches, pancreatic cancer is usually diagnosed at advanced incurable stages [2]. In addition, extensive local tumor invasion and systematic metastasis were frequently observed in advanced PDAC, limiting therapeutic options for PDAC patients [3]. Despite the fact that vigorous efforts have been made to improve the therapeutic options of PDAC patients, the prognosis of PDAC remains largely unchanged in the last two decades [4]. Growing evidence supports the existence of cancer stem-like cells (CSLCs) within pancreatic tumors and the importance of CSLCs in PDAC progression and metastasis, highlighting the pathological significance of CSLCs in PDAC diagnosis and treatment [5, 6]. For

example, transcription factors Oct4 and Nanog play indispensable roles in the pluripotency and self-renewal of embryonic and somatic stem cells. Likewise, Oct4 and Nanog are compulsively requested for maintaining CSLC phenotypes [7]. Both of Oct4 and Nanog are significantly upregulated at early stages of PDAC and are associated with dismal prognosis of PDAC [8]. However, the mechanisms leading to pancreatic CSLCs remain poorly understood.

It has recently become clear that epithelial-mesenchymal transition (EMT) is closely associated with cancer stemness and chemoresistance [9]. During the process of EMT, the expression of epithelial marker proteins, such as E-cadherin and ZO-1, decline, while the expression of mesenchymal markers, including vimentin, N-cadherin, fibronectin and twist, are up-regulated [10]. The expression of EMT marker proteins is largely governed by EMT-related transcription factors, especially snail and slug. The activation of Snail and slug plays central roles in the initiation of EMT process [11]. Snail and Slug directly activate the transcription of mesenchymal marker proteins and repress the expression of epithelial markers, rendering the initiation of EMT. Recent studies have indicated that EMT plays important roles in stem cell-like characteristics of tumor cells [12, 13]. Nevertheless, the precise mechanisms underlying the transformation between EMT-phenotype and CLSCs remain to be elucidated [14, 15]. In PDAC cells, it was reported that EMT process dramatically enhanced migratory and invasive capacities of CLSCs [16]. Polyak et al indicated that EMT is a key process for PDAC cells to obtain and maintain stemness characteristics of CSLCs during pancreatic tumorigenesis. They detected phenotype alterations in a small group of PDAC cells which lost epithelial features and gained mesenchymal features, and found that these cells exhibited CSLC phenotypes and became very aggressive [17]. AV Salnikov reported that hypoxia-induced EMT phenotype promoted pronounced migratory potential in pancreatic CSLCs, and this effect did not occur in normal tumor cells. These findings suggest a close relationship between EMT and CLSC phenotypes during PDAC development.

Mounting studies have revealed that microRNAs (miRNAs) are key players of carcinogenesis. MiRNAs are short non-coding RNAs and mainly function through modulating the translation and decay of mRNAs [18]. Recently, emerging evidence pointed to a pivotal role of miRNAs in the regulation of EMT process in tumor cells [19]. JP Zhang reported that microRNA-148a

impeded EMT process through targeting c-MET mRNA [20]. The miR-30 family contains five subtypes: miR-30a, b, c, d, e, and they have been proved to act as tumor suppressors in various types of malignant tumors, such as breast cancer, non-small cell lung cancer (NSCLC), renal carcinoma and gastrointestinal cancer. Low levels of miRNA-30 members are closely related with highly aggressive behaviors of various cancers [21-23]. Increasing evidence suggests that miR-30 family members may play crucial roles in tumor initiation and progression through regulating EMT process [24]. Recent studies have reported that the levels of miR-30 family members were significantly down-regulated in Lin-28^{+} CSLCs, compared to Lin-28[-]cells [25]. Another study has shown that breast CSLCs expressed remarkably low levels of miR-30a, b, c, and d, compared with normal breast cancer cells. Furthermore, recent investigations showed that CSLCs derived from PDAC cell line MiaPaCa-2 (CD44^{+}, CD133^{+}, EpCAM^{+}) exhibited reduced levels of miR-30a and miR-30c, compared to both parental MiaPaCa-2 cells and triple-negative (CD44^{-}, CD133^{-}, EpCAM^{-}) cells [26]. These findings suggest that miR-30 family members may negatively regulate EMT and CSLCs.

In the present study, we investigated the roles of miR-30 members in EMT phenotype of PCSCs. We firstly reported that miR-30b impeded EMT process of PCSCs by directly targeting Snail. To some extent, our findings highlight that miR-30b analogs might be served as a novel therapeutic agent for PC by suppressing EMT-phenotype of PCSCs.

Materials and Methods

Cell culture

Human pancreatic ductal adenocarcinoma cell line PANC-1 was obtained from Chinese Academy of Sciences (Shanghai, China). Cells were cultured in DMEM medium supplemented with 10% fetal bovine serum (FBS; Hyclone, Shanghai) at 37°C in a humidified 5% CO_2 incubator (Thermo Fisher Scientific Inc., UK). PCSCs sorted from PANC-1 cells were cultured in DMEM-F12 supplemented with 1% N2 Supplement (Invitrogen, USA), 2% B27 Supplement (Invitrogen), 20 ng/ml human platelet growth factor (Sigma-Aldrich, USA) and 100 ng/ml epidermal growth factor (Invitrogen).

Fluorescence activated cell sorting of PCSCs

First, PANC-1 cells were washed once with phosphate buffer saline (PBS) containing 3% fetal calf serum (FCS)). Then, Fc receptor was blocked using FcR Blocking Reagent on ice for 10-15 minutes. Thereafter, PANC-1 cells were incubated for 30

minutes at 4°C in dark with the following monoclonal antibodies: anti-human CD24-PE (Becton Dickinson, USA) (1:40), anti-human CD44-APC (Becton Dickinson, USA) (1:40) and anti-human EpCAM-FITC (Becton Dickinson, USA) (1:40). Next, cells were washed twice with PBS and resuspended in culture medium. Subsequently, cells were subjected to flow cytometrical analysis on a flow cytometer (FACS Aria II, USA). Cells were sorted twice and reanalyzed, exceeding a purity of 95%. BD FACS Diva software were used to analyze the data.

MiR-30b mimic transfection

MiR-30b mimic and NC mimic were designed and synthesized by Ribo-Bio Co Ltd (Guangzhou, China). PCSCs were seeded in 6 well plates and incubated overnight, reaching 40% to 50% confluence, and then transiently transfected with 100 nM miR-30b mimic or NC mimic using riboFECT™ CP Transfection Reagent (Ribo-Bio Co Ltd., China). 24 h after transfection, cells were harvested for subsequent experiments.

RNA extraction and RT-qPCR

Total RNA was extracted from cells treated with Trizol Reagent (Invitrogen, USA) in accordance with manufacturer's instrument. Rayscript cDNA Synthesis Kit (Ceneray, China) was used to synthesize the first-strand cDNA. RT-qPCR was performed using a qPCR PreMix Kit (Ceneray, China) on ABI7900 Real-time PCR System (Thermo Fisher Scientific Inc., UK). MiR-30s were normalized to small nuclear U6. Oct4, Nanog, E-cadherin, vimentin, N-cadherin and Snail were normalized to GAPDH. Relative quantification of gene expression was calculated automatically using $2^{-\Delta\Delta Ct}$. PCR primer sequences were designed and synthesized by Generay Co Ltd (Shanghai, China).

Western blot analysis

Cells were lysed in RIPA lysis buffer (Solarbio, China) supplemented with 1% PMSF (Solarbio, China). Protein concentration was determined using Enhanced BCA Protein Assay Kit (Beyotime, China). Equal amount of protein sample was separated on 10 % SDS-PAGE and transferred to polyvinylidene difluoride (PVDF) membranes (Solarbio, China). The membranes were blocked in 5% BSA buffer (Solarbio, China) and then incubated with primary antibodies (Rabbit anti-Oct4, 1:1000, Abcam; Rabbit anti-Nanog, 1:1000, Abcam; Rabbit anti-N-cadherin, 1:5000, Abcam; Rabbit anti-E-cadherin, 1:10000, Abcam; Rabbit anti-vimentin, 1:1000, Abcam; Rabbit Anti-Snail, 1:1000, Cell Signaling; Rabbit Anti-GAPDH, 1:10000, Abcam) overnight at 4°C or for

2 h at room temperature. After three times of washes, the membranes were incubated with horseradish peroxidase-conjugated secondary goat anti-rabbit antibodies (1:4000; Biosharp, China) for 1 h at room temperature according to the manufacturer's instructions. The detection of immunocomplexes was performed with an enhanced chemiluminescence system (NEN Life Science Products, USA). The experiments were carried out on three separate occasions.

Transwell migration and invasion assay

5×10^5 PCSCs were seeded onto the non-coated membrane (24-well insert; pore size, 8μm; Corning Costar, USA) (for migration assay) or Matrigel (60mg/well; BD Bioscience, USA) coated membrane (for invasion assay) in the top chamber using serum-free DMEM medium. Medium supplemented with 5% FBS, providing a chemotactic function, was added to the lower chamber. After incubated for 24 hours (for migration assay) or 36 hours (for invasion assay), cells that did not migrate/invade through the membrane were removed by a cotton swab. Cells on the lower surface of the membrane were fixed with 4% paraformaldehyde and stained with 0.1% crystal violet. The number of cells migrated/invaded through the membrane was counted under microscope (five random fields per well).

Luciferase reporter assay

The 3'UTR sequence of human Snail gene containing predicted binding site for miR-30b was amplified by PCR using PANC-1 cell genomic DNA as a template. PCR primer sequences are 5'-CCC AAG CTT GGG GGG ACT GTG AGT AAT GGC TG-3' (forward) and5'-CGA GCT CGA ACG TTT CCT TGA TAC AAA ATG T-3' (reverse). Snail wild-type (WT-3'UTR) vector was constructed by inserting the PCR fragment into pMIR-REPORT luciferase vector (Ambion, USA). Mutant vector (MUT-3'UTR) was constructed using an overlap extension method. Cells were planted into 24-well plate at 50–60% confluency. 24 h later, cells were transfected with pRL-TK vector (20ng) and WT-3'UTR or MUT-3'UTR vectors (180ng), along with miR-30b mimic or NC mimic at a concentration of 100 nM using riboFECT™ CP Transfection Reagent (Ribo-Bio Co Ltd., China). Each group is composed of three duplicate wells. 24 hours after transfection, the relative firefly luciferase activity (normalized to Renilla luciferase activity) was measured using a dual-luciferase reporter gene assay system (Promega, USA), and results were depicted as fold changes relative to respective controls.

MiR-30b lentiviral infection

MiR-30b was subcloned into a H1-miRNA-CMV-Puromycin lentiviral vector Genechem (Shanghai, China). Subsequently, miR-30b-overexpressing and NC lentiviruses were packaged by Genechem. PCSCs were seeded in 6-well ultra-low attachment culture dishes, incubated overnight and then infected with miR-30b-overexpressing or NC lentiviruses. 48 h after infection, the expression of miR-30b was examined using RT-qPCR analysis.

In vivo tumorigenicity assay

1×10^5 of PCSCs were injected subcutaneously into the flanks of 4-week-old male Balb/c athymic nude mice (n = 6 per group). Mice were monitored every three days and euthanized four weeks later. Tumors were dissected and weighed, and tumor volume was calculated as V (volume, mm^3) = 0.5×L (length, mm) × W^2 (width, mm^2). Animal experiments were performed using protocols approved by the Animal Center of the Medical College of Soochow University.

Immunohistochemistry and tissual miR-30b expression analysis

100 PDAC tissues with follow-up data were obtained from Surgical department of First Affiliated Hospital of Soochow University. The tissues were processed into tissue microarrays. The tissue microarrays were deparaffinized using a graded ethanol series and endogenous peroxidase activity was blocked by soaking in 0.3% hydrogen peroxide. Thereafter, the tissue microarrays were processed in 10 mM citrate buffer (pH 6.0) and heated to 121 °C in an autoclave for 5 minutes to retrieve the antigen. After rinsing in phosphate-buffered saline (PBS; pH 7.2), 10% goat serum was applied for 1 hour at room temperature to block any non-specific reactions. A tissue microarray was then incubated over night with mouse anti-human Snail monoclonal antibody (diluted 1:800; Abcam, USA). Negative control tissue microarray was also processed in parallel using a non-specific immunoglobulin IgG (diluted 1:100; Santa Cruz Biotechnology) at the same concentration as the primary antibody. All tissue microarrays were processed using the peroxidase-anti-peroxidase method (Dako, Hamburg, Germany). After rinsing in water, the peroxidase tissue microarrays were counterstained with hematoxylin, dehydrated, and cover-slipped.

For the evaluation of miR-30b expression, PDAC tissues were subjected to RNA extraction in a high-throughput manner using RNeasy 96 Universal Tissue Kit (Qiagen, Shanghai, China) in accordance with the manufacture's instruments. Subsequently, cDNA was reverse-transcribed using a ReverTra Ace reverse transcription kit (Toyobo, Shanghai, China) and subjected to miR-30b expression detection using SYBR RT-qPCR assay.

Immunohistochemical evaluation

Stained tissue microarrays were observed under a microscope. All the immunostained tissue microarrays were evaluated in a blinded manner without knowledge of the clinical and pathological parameters of the patients. For assessment of Snail, 5 high-power fields in each specimen were selected randomly, and cell staining was examined under high-power magnification. More than 500 cells were counted to determine the mean percent, which represented the percentage of immunostained cells related to the total number of cells. The staining of Snail was scored as 0 (no expression), 1 (weak expression), 2 (moderate expression) and 3 (strong expression). Then, each specimen was assigned with a final expression score through multiplying staining score and percentage of expression. The evaluation of Snail expression was performed independently by two pathologists to avoid possible technical errors, and high consistencies were obtained in these samples (kappa coefficient: 0.97).

Statistical analysis.

Data were analyzed using STATA 11. Results were expressed as mean ± S.E. and presented using GraphPad Prism 7 software (GraphPad Software, Inc., USA). Each experiment was repeated at least three times per condition. MiR-30b and Snail expression in PDAC was studied using the Spearman rank correlation test because the data were not normally distributed. The association between miR-30b/Snail expression and clinicopathological features were computed using the Pearson χ2 test. P<0.05 was considered statistically significant.

Results

Isolation and characterization of PCSCs.

To decipher the molecular mechanisms underlying PCSCs, PANC-1 cells were subjected to flow cytometry analysis to isolate PCSCs using three well-characterized PCSC markers, CD24, CD44 and EpCAM [27]. As shown in Fig. 1A and 1B, 6.02%-9.81% of PANC-1 cells were double-positive (CD24$^+$, CD44$^+$), and 4.52%-8.09% were triple-positive (CD24$^+$, CD44$^+$, EpCAM$^+$). The morphologies of normal PANC-1 cells and triple-positive PCSCs were shown in Fig. 1C and 1D. Triple-positive PCSCs formed spheroids in an ultra-low attachment culture dish (Fig. 1D). As mentioned in introduction section, Oct4 and Nanog play indispensable roles in

maintaining the pluripotency of embryonic stem cells and tumor-initiating property of CSLCs [7]. Therefore, we examined the expression of Oct4 and Nanog in PCSCs. RT-qPCR and western blot analyses were performed to evaluate mRNA and protein levels of Oct4 and Nanog in PCSCs. As shown in Fig. 1E-G, Oct4 and Nanog expression were significantly increased at both mRNA and protein levels in PCSCs, compared with normal PANC-1 cells.

Expression of miR-30 family and EMT markers in PCSCs.

To explore the expression profiles of miR-30 members in PCSCs and its relationship with EMT markers, RT-qPCR was performed to determine the mRNA levels of miR-30 family members and EMT markers in normal PANC-1 cells and PCSCs. In addition, western blot analysis was carried out to determine the expression of EMT markers in PANC-1 cells and PCSCs at protein level. The results showed that expression levels of miR-30b, c, d were significantly downregulated in PCSCs, while the level of miR-30a, were largely unchanged between PCSCs and normal PANC-1 cells (Fig. 2A). Moreover, we found the expression of N-cadherin and vimentin were upregulated, while E-cadherin exhibited significant down-regulation at both mRNA and

protein levels in PCSCs (Fig. 2B-D). These results suggested that PCSCs showed EMT characteristics and miR-30 family members could be potential regulators of EMT phenotypes of PCSCs.

MiR-30b negatively regulates EMT process and partially reduced the stemness of PCSCs.

Because miR-30b displayed the most significant reduction among the total 5 members of miR-30 family in PCSCs (Fig. 2A), we focused on the role of miR-30b in the regulation of PCSCs. After transfected with miR-30b mimic or NC microRNA, PCSCs were subjected to RNA isolation and RT-qPCR analysis. As shown in Fig. 3A, transfection with miR-30b mimic remarkably increased the level of miR-30b in PCSCs (Fig. 3A). Thereafter, we performed RT-qPCR and western blot analysis to determine the mRNA and protein levels of EMT markers. We found that overexpression of miR-30b resulted in significant up-regulation of epithelial marker E-cadherin and down-regulation of mesenchymal marker N-cadherin at both mRNA and protein levels (Fig. 3B-D), while the expression of vimentin appeared unchanged. These results indicated that the down-regulation of miR-30b is an important step for tumor cells to obtain EMT features, whereas enforced expression of miR-30b may suppress the EMT process of PCSCs.
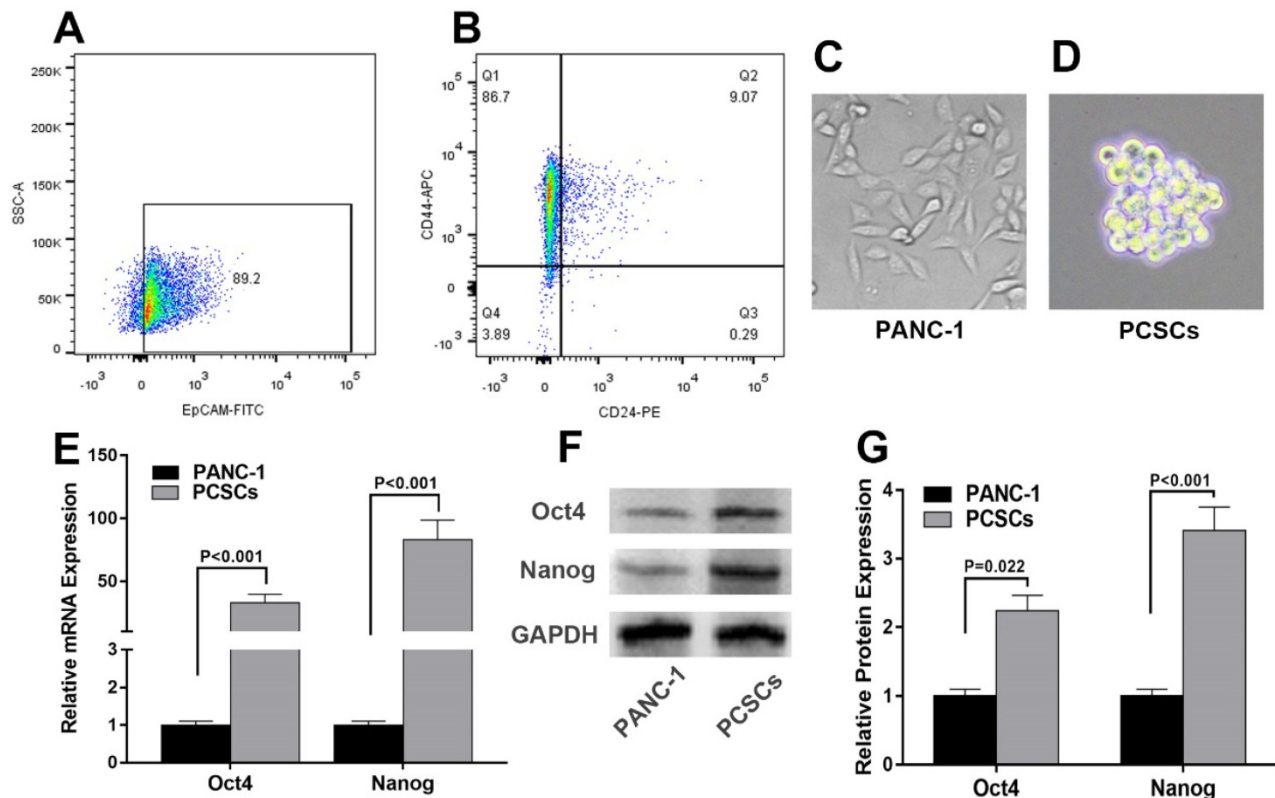

Figure 1. Isolation and characterization of Triple-positive (CD24, CD44, EpCAM) PCSCs sorted from PANC-1 cells. Flow cytometric analysis was employed to sort triple-positive PCSCs in PANC-1 cells. (A) EpCAM+ population of PANC-1 cells. (B) CD24+ CD44+ population of sorted EpCAM+ PANC-1 cells. (C and D) The morphologies of PANC-1 cells and PCSCs. (E) mRNA levels of Oct4 and Nanog were measured using RT-qPCR analysis in normal PANC-1 cells and PCSCs. (F and G) Western blot analysis of Protein levels of Oct4 and Nanog in PANC-1 and PCSCs. Data are means ± S.E. of three independent experiments.
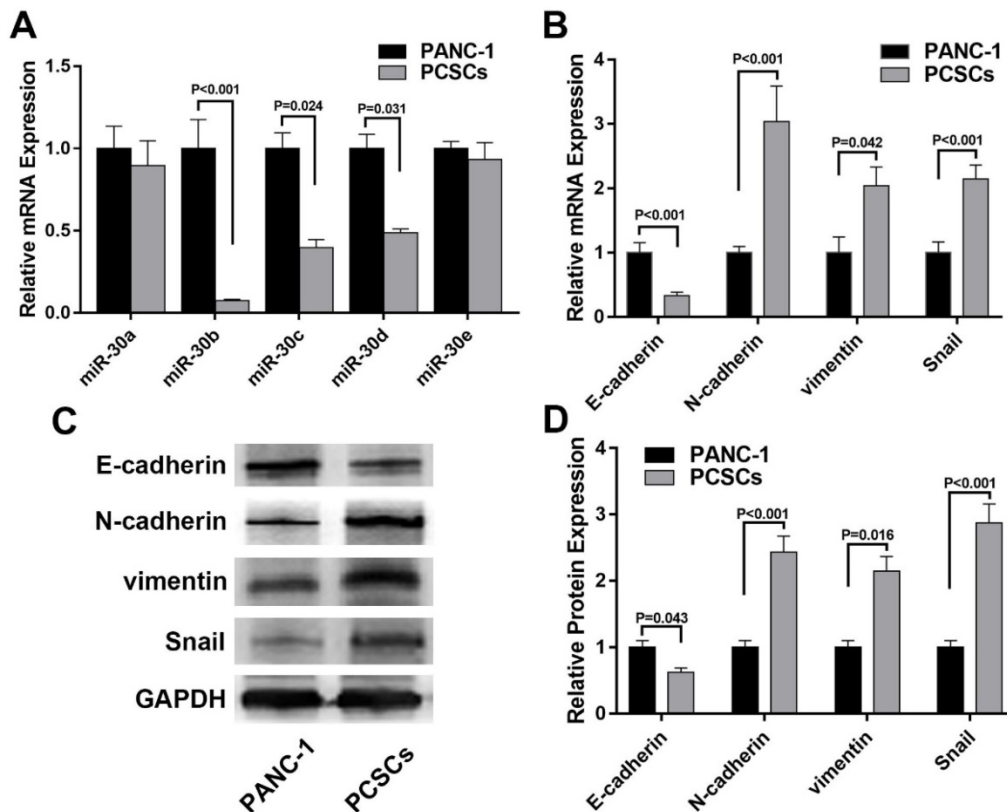
Figure 2. miR-30s and EMT markers are differentially expressed in PANC-1 cells and PCSCs. (A and B) mRNA levels of miR-30s and EMT markers measured by RT-qPCR in PANC-1 cells and PCSCs. (C and D) Protein expressions of EMT markers were determined using western blot analysis in PANC-1 cells and PCSCs. Data are the means ± S.E. of three independent experiments.

Moreover, the morphology of PCSCs changed from compact sphere to unconsolidated cell clusters following miR-30b overexpression, indicating that miR-30b might inhibit stemness of PCSCs (Fig. 3E-G).

MiR-30b overexpression reduces the migration and invasion of PCSCs.

EMT-phenotype is associated with more aggressive and metastatic capacity compared to normal cancer cells [28]. We used transwell assay to evaluate the influence of miR-30b on migratory and invasive features of PCSCs. Overexpression of miR-30b mimics significantly impaired the migration and invasion of PCSCs, as indicated by the fact that the number of PCSCs migrated or invaded through the membrane was notably decreased in miR-30b-overexpressing PCSCs, compared with untreated PCSCs or PCSCs transfected with NC mimic (Fig. 4). Combined the results above, we speculated that enforced expression of miR-30b reduced migratory and invasive capacities of PCSCs by suppressing EMT process.

MiR-30b directly targets Snail in PCSCs.

To explore the mechanism by which miR-30b suppressed EMT process of PCSCs, we explored potential target genes of miR-30b. Using TargetScan

(http://www.targetscan.org/) and PicTar (pictar .mdc-berlin.de/), we found that the 3' UTR of Snail mRNA contains a putative binding site of miR-30b (Fig. 5A). To determine whether miR-30b may regulate Snail expression through directly binding to the putative binding site of Snail mRNA 3' UTR, we subcloned Snail mRNA 3' UTR sequence into a luciferase reporter construct (designated as Snail WT-3'UTR). In addition, we mutated the putative miR-30b binding site (designated as Snail MUT-3'UTR). Next, luciferase reporter assay was performed to validate whether miR-30b can inhibit the reporter activity of Snail 3' UTR. NC mimic or MiR-30b mimic was co-transfected with Snail WT-3'UTR or Snail MUT-3'UTR construct and a Renilla-luciferase control reporter vector into PCSCs. As shown in Fig. 5B, compared with NC mimics, miR-30b mimics significantly decreased the luciferase activity of Snail WT-3'UTR. However, miR-30b mimics had no significant influence on the luciferase activity of the Snail MUT-3'UTR (Fig. 5B). Next, we analyzed the influence of miR-30b on mRNA and protein expression of Snail. As predicted, overexpression of miR-30b mimics led to decreased expression of Snail both at mRNA and protein levels (Fig. 5C-E). Taken these results together, we conclude that miR-30b may suppress the expression of Snail by
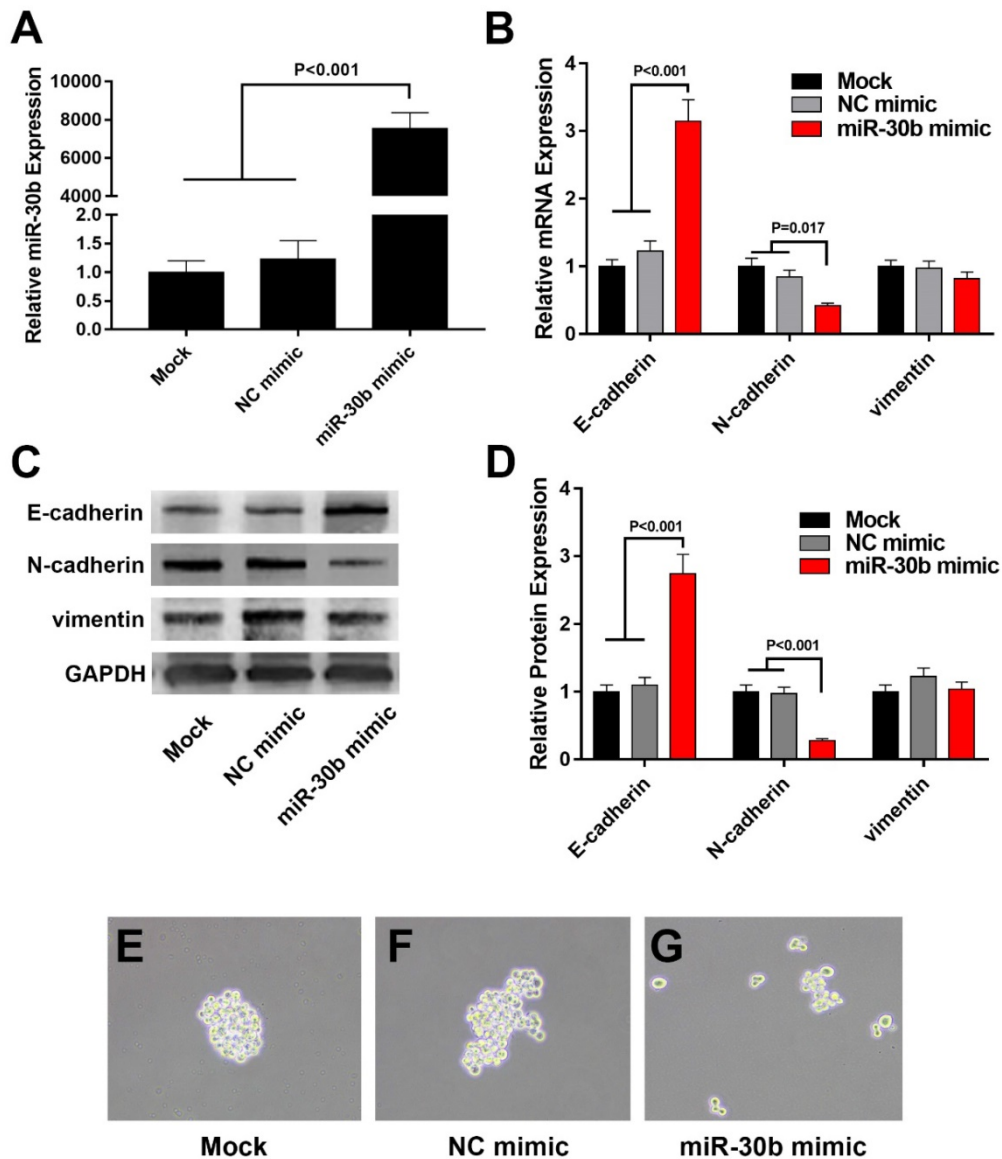
Figure 3. Overexpression of miR-30b impairs EMT process in PCSCs. (A) qRT-PCR analysis of miR-30b expression in PCSCs transfected with NC mimic or miR-30b mimic. (B) The mRNA levels of EMT makers was determined using qRT-PCR analysis in control and miR-30b-overexpressing PCSCs. (C and D) Western blot analysis of the expression of EMT makers in PCSCs following the transfection of NC mimic or miR-30b mimic. (E-G) The morphologies of mock-treated PCSCs and PCSCs transfected with NC mimic or miR-30b. Data are means ± S.E. of three independent experiments.

directly binding to the 3'UTR of Snail mRNA, consequently leading to Snail downregulation and inhibiting the EMT process of PCSCs.

MiR-30b overexpression impairs the tumorigenic capacity of PCSCs in *vivo*.

Next, the effect of miR-30b on in vivo tumorigenic capacity of PCSCs was examined. To this end, PCSCs were infected with miR-30b-overexpressing or NC lentiviruses. The expression of miR-30b in miR-30b-overexpressing PCSCs was verified using RT-qPCR analysis (Fig. 6A). Thereafter, PCSCs were injected subcutaneously into the flanks of Balb/c athymic nude mice and tumor growth was examined. As shown in Fig. 6B, miR-30b overexpression efficiently impaired *in vivo*

tumorigenic capacities of PCSCs. Moreover, the volumes and weights of miR-30b0-overexpressing tumors were significantly decreased as compared to mock and NC groups (Fig. 6C and 6D).

The correlation of miR-30b and Snail expression with clinicopathological factors in PDAC patients.

To determine whether the expression levels of miR-30b and Snail protein are associated with the histological characteristics of PDAC, tissue microarrays containing 100 paraffin-embedded, achieved PDAC clinical specimens with follow-up data, were examined using immunohistochemical analysis. Snail expression was scored in each PDAC specimen (Fig. 7A-D). In addition, relative expression
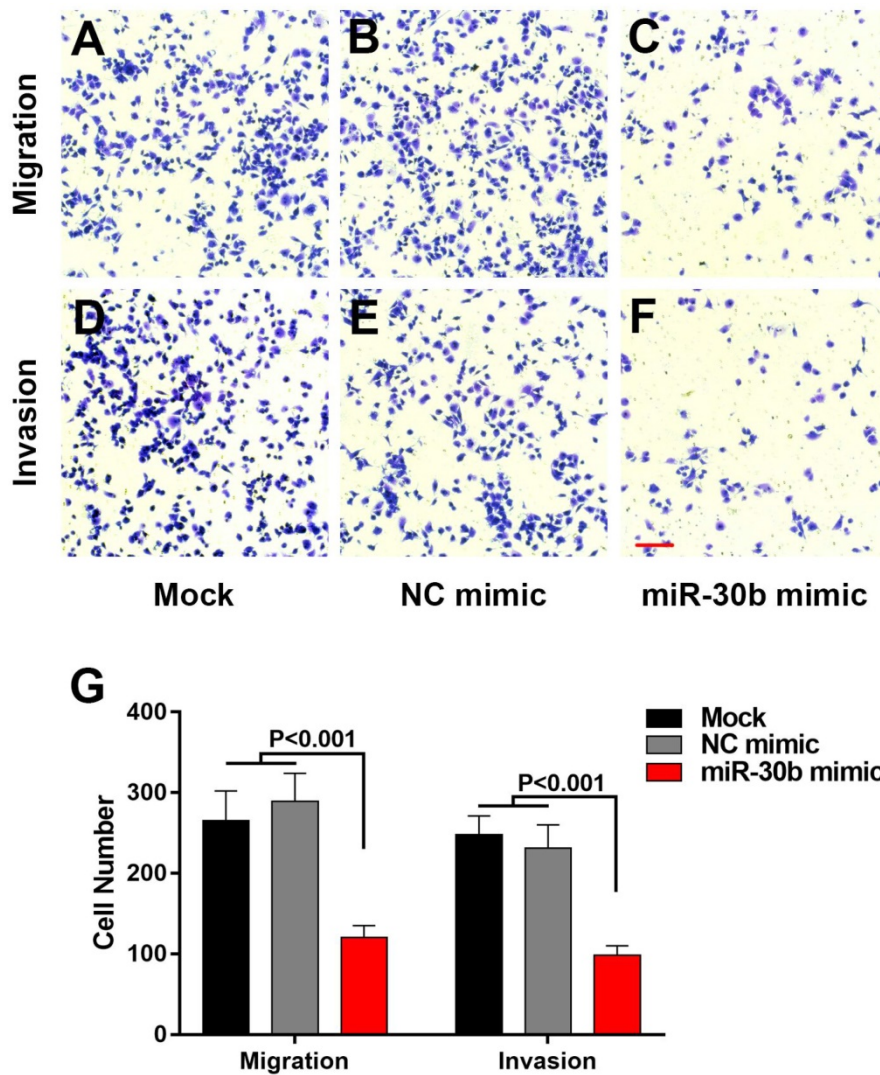
Figure 4. MiR-30b remarkably inhibits the migration and invasion of PCSCs (A-F) The capacities of PCSCs mock-transfected, transfected with NC mimic or miR-30b mimic were determined using Transwell migration assay or matrigel transwell assay, respectively (Scale bar=50μm). (G) Quantitative analysis of migratory and invasive capacities of each group of PCSCs. Data are means ± S.E.

of miR-30b was evaluated using RT-qPCR analysis. In this way, we observed an inverse correlation between miR-30b and Snail expression, with a co-efficient of -0.391 (Fig. 7E). The patients' clinicopathological data are summarized in Table 1. As shown in Table 1, we evaluated the association of miR-30b and Snail expression levels with clinicopathological parameters. There was no significant correlation between miR-30b expression and the prognostic factors such as patients' age, gender, and tumor size, while miR-30b expression was significantly correlated with neuro invasion (P=0.018), TNM stage (P<0.001), tumor differentiation (P<0.001) and Snail expression level (P<0.001). Likewise, we found that Snail expression was significantly correlated with TNM stage (P=0.001) and tumor differentiation (P=0.016), but not with other prognostic factors, including patients' age, gender, tumor size and neuro invasion.

Prognostic significance of miR-30b and Snail expression in PDAC patients.

Because follow-up data were obtained in these patients, we analyzed whether Snail and miR-30b expression could influence the prognosis of PDAC patients. Indeed, low expression of miR-30b is strongly associated with dismal prognosis in PDAC patients (Fig. 8A). Similarly, high expression of Snail (cut-off=1.55) strongly predicts worsened survival, as compared with patients with low Snail expression (Fig. 8B). Moreover, when comparing patients with low miR-30b expression plus high Snail expression and other patients, we found that these patients exhibited markedly unfavorable survival compared with other patients (Fig. 8C). These findings explicitly demonstrate that miR-30b-mediated Snail regulation plays a crucial role in suppressing malignant development of PDAC.
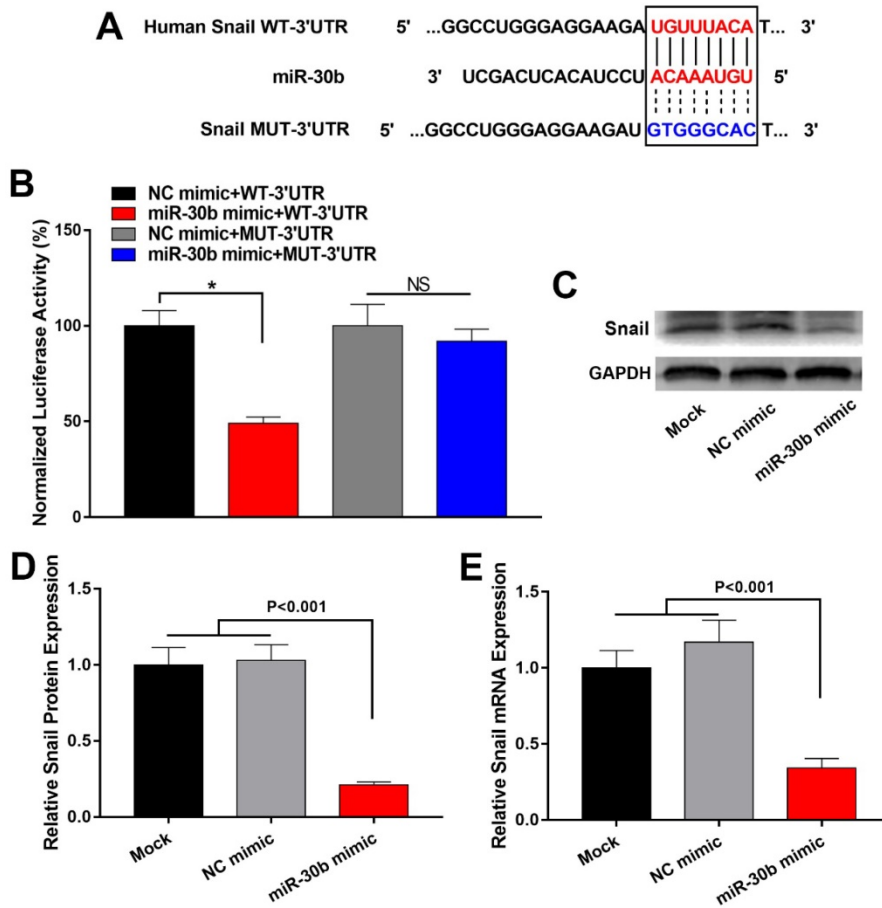
Figure 5. MiR-30b directly targeted Snail in PCSCs. (A) Predicted miR-30b targeting sequence in 3′ UTR of Snail (Snail WT-3'UTR) and mutant form of Snail 3' UTR construct (Snail MUT-3'UTR). (B) Luciferase reporter assay was conducted to determine the influence of miR-30b on Snail 3'UTR activity in PCSCs. PCSCs were transfected with WT-3'UTR or MUT-3'UTR and NC mimic or miR-30b mimic. 24 h after transfection, cells were harvested and subjected to luciferase reporter assay. Data are the means ± S.E. of three independent experiments. (C and D) Transfection of miR-30b impaired mRNA and protein levels of Snail in PCSCs.
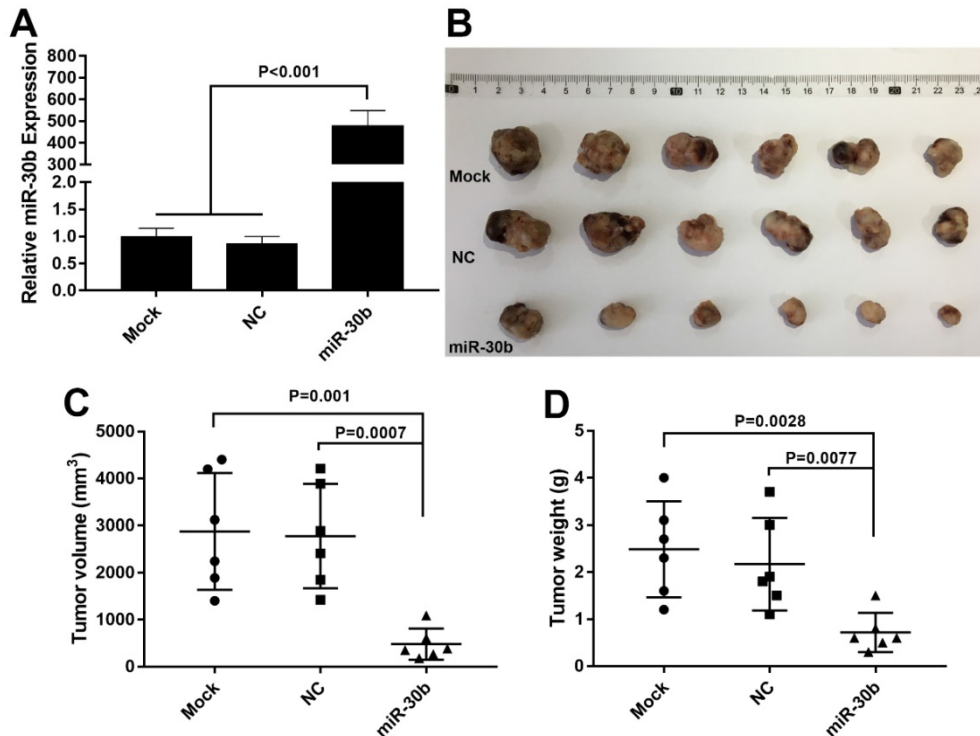

Figure 6. MiR-30b overexpression suppresses tumorigenic potential of PCSCs *in vivo*. (A) RT-qPCR analysis of miR-30b expression in PCSCs 48 h after infection with NC or miR-30b-overexpressing lentiviruses. (B-D) Size, volume, and weight of tumors derived from mock, NC or miR-30b-overexpressing PCSCs.
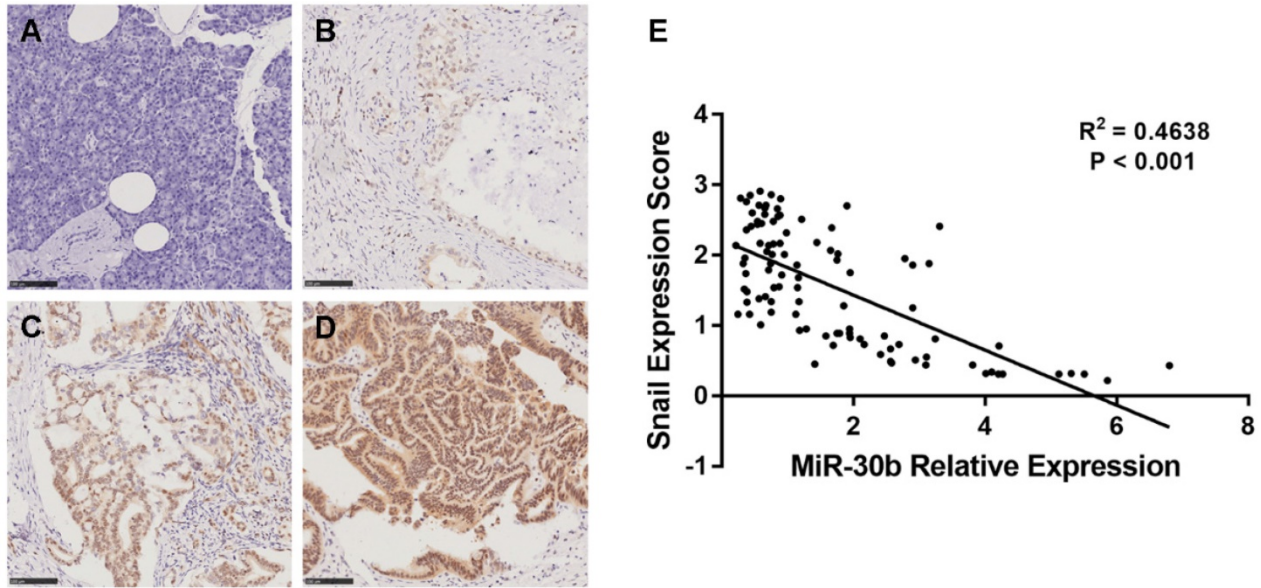
Figure 7. Relationship between miR-30b relative expression and Snail expression score in PDAC. (A-D) Representative images of Snail imunohistochemtry in non-tumorous pancreatic (A) and PDAC specimens (B-D). A, non-tumorous pancreatic tissue; B, weak expression; C, moderate expression; D, strong expression. (E) Scatterplot of miR-30b versus Snail with regression line showing a correlation of them using the Spearman's correlation coefficient. (Scale bar=100μm)
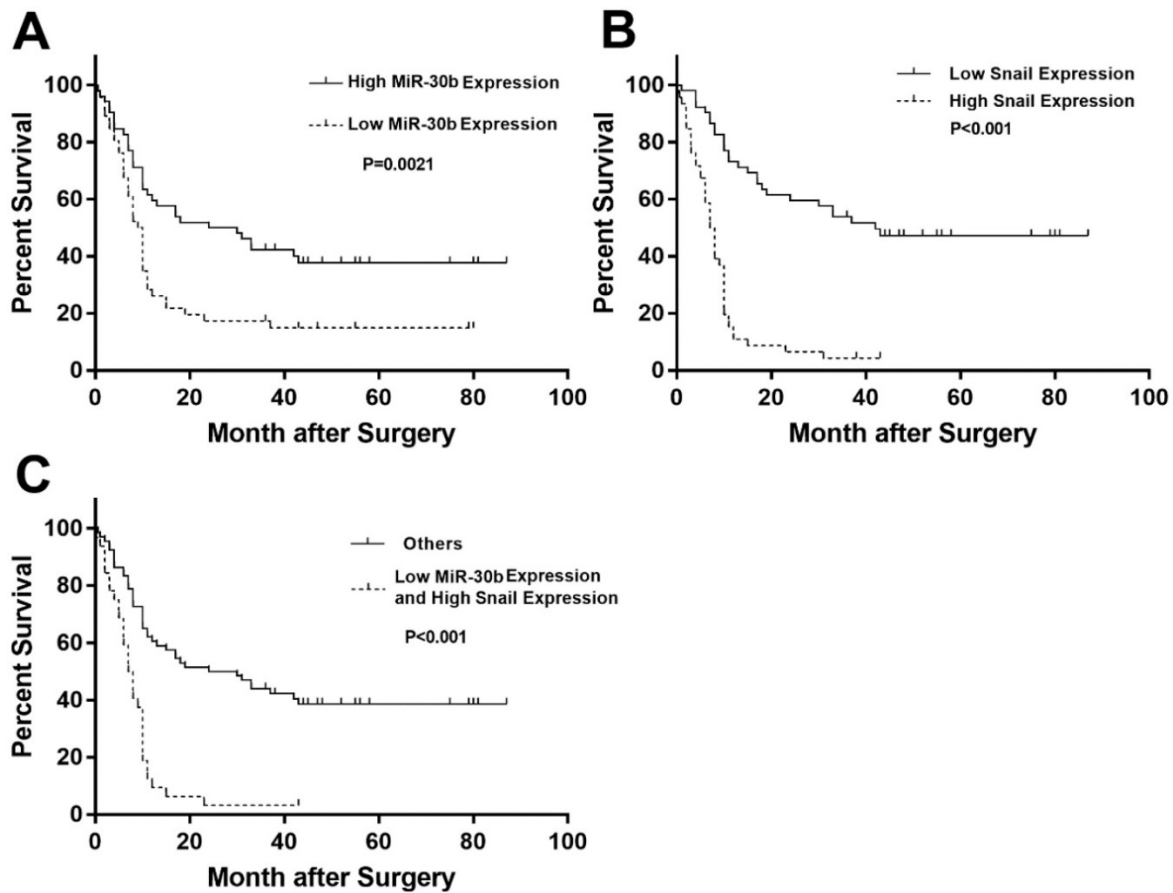

Figure 8. Prognostic significance of miR-30b and Snail expression. (A) Kaplan–Meier survival curves of high miR-30b expression versus low miR-30b expression in 100 patients of PDAC showed a highly significant separation (P=0.0021). (B) Kaplan–Meier survival curves of low Snail expression versus high Snail expression in 100 patients of PDAC showed a highly significant separation (P<0.001). (C) Kaplan–Meier survival curves of low miR-30b expression and high Snail expression versus others in 100 patients of PDAC showed a highly significant separation (P<0.001).

Table 1. Clinicopathological features of PDAC in relation to the MiR-30b/Snail expression pattern

Clinicopathological Features		MiR-30b			Snail		
		Low	High	*P* Value	Low	High	*P* Value
Age(years)	≤62	26	24	0.423	28	22	0.423
	>62	22	28		24	26	
Gender	female	16	21	0.466	20	17	0.753
	male	32	31		32	31	
Maximal Tumor Size(cm)	≤4.0	24	36	0.084	34	26	0.369
	>4.0	22	16		18	20	
Neuro Invasion	absent	23	37	0.018*	28	32	0.191
	present	25	15		24	16	
TNM Stage	I	8	32	<0.001*	30	10	0.001*
	II	38	19		22	35	
	III	0	0		0	0	
	IV	2	0		0	2	
Differentiation	poor	25	7	<0.001*	11	21	0.016*
	well	23	45		41	27	
Snail Expression	low	14	38	<0.001*			
	high	34	14				

Statistical analyses were carried out using Pearson χ² test. * P<0.05 was considered significant

Discussion

PDAC is the fourth leading cause of cancer-related mortality in western countries. The prognosis of PDAC is extremely unfavorable with an overall 5-year survival of 5% and a median survival period of less than 6 months [29]. The term cancer stem-like cells (CSLCs) was adopted in early 2000s to define a small population of cancer cells with potential of indefinite self-renewal that drive carcinogenesis [30]. As such, CSLCs are widely regarded as an important target for novel anti-cancer treatment. Recently, microRNAs have been suggested to play crucial roles in EMT and malignant behaviors of CSLCs [31, 32]. These findings implicate that microRNAs may serve as promising therapeutic agents in targeting CSLCs and cancer treatment.

CSLCs were initially characterized by their property to self-renew and differentiate into all malignant populations [33]. However, studies over the last decade have explicitly demonstrated a pivotal role of CSLCs in tumor chemoresistance and metastasis [34]. In addition, mounting investigations suggested that EMT phenotype plays a crucial role in CSLC malignancy, chemoresistance and metastasis [35]. For example, overexpression of snail triggers EMT program and CSLC phenotype in colon cancer cells, which contributes to chemoresistant to oxaliplatin [36]. In addition, AKT/β-catenin-mediated activation of Snail expression promotes acquisition of EMT phenotype and CSLC features in cisplatin-resistant lung cancer cells [37]. Of great intrigue, multiple studies revealed that microRNAs play important roles in the upregulation of Snail in tumor cells. Helge Siemens et al reported that miR-34 targeted Snail to suppress EMT and tumor metastasis [38]. It was also reported that miR-22 may inhibit gastric tumor growth and metastasis through targeting Snail and MMP14 [39]. However, the regulation of Snail in pancreatic cancer remains largely obscure. In the present study, we revealed that miR-30b may suppress Snail expression through directly targeting Snail mRNA 3' UTR. Through the regulation of Snail, miR-30b promotes the expression of E-cadherin but impairs the level of N-cadherin in PCSCs, indicating that miR-30b suppresses EMT process in PCSCs through posttranspritionally modulating Snail expression.

In recent years, the biological functions of miRNAs have been widely reported, especially in oncology field. Members of miR-30 family have been suggested to function as tumor suppressors, and have been reportedly downregulated in various tumor types, including breast cancer, NSCLC, renal carcinoma, gastrointestinal cancer [21-23, 40-42]. The levels of miR-30s have been shown to be closely associated with EMT process of diverse tumorous or non-tumorous cells [43-45].Thus, the molecular link between miR-30 family and EMT process in PDAC is a topic of investigation, and the clarification of their roles may benefit the development of novel therapeutic strategies for the treatment of PDAC. The initial aim of our study was to determine the roles of miR-30s in the maintenance of PCSCs. Unexpectedly, we uncovered an involvement of miR-30b in the regulation of Snail expression and EMT process. miR-30b directly binds to Snail 3'UTR and inhibits Snail translation. Forced expression of miR-30b impaired the expression of Snail but promoted the expression of epithelial marker E-cadherin. In addition, we revealed that miR-30b expression is negatively correlated with the level of Snail in PDAC patients. More importantly, patients with low miR-30b level and high Snail expression displayed markedly unfavorable survival, compared with other patients. These findings implicated that overex-

pression of miR-30b may inhibit both stemness phenotype and EMT process of PDAC, highlighting the therapeutic merit of miR-30b in PDAC treatment.

In summary, we isolated a highly tumorigenic subpopulation in PDAC cell line PANC-1 with stem-like characteristics through their expression of cell surface markers CD24, CD44 and EpCAM. In addition, we revealed that miR-30b played an important role in suppressing EMT process and cell invasion in PCSCs. Moreover, we provided evidence that miR-30b directly target Snail to impede the EMT process of PCSCs. Our findings provide a novel insight into the mechanism by which miR-30b regulates EMT process during PDAC development and metastasis. These results indicate that miR-30b and its analogs may serve as promising therapeutic agents to reverse EMT-phenotype in PCSCs and selectively eliminate PCSCs.

Abbreviations

PDAC: Pancreatic ductal adenocarcinoma; PCSC: Pancreatic cancer stem cell; EMT: epithelial-mesenchymal transition; MET: mesenchymal-to-epithelial transition; CSLC: Cancer stem-like cell; MiR: MicroRNA.

Acknowledgments

Additional Information

Yicheng Xiong and Yao Wang contributed equally to this work.

Contributions: The study was conceived by Yicheng Xiong, and designed byYicheng Xiong, Haixin Qian, Yao Wang, Mingyan Zhu and Lei Wang. Experiments were performed by Yicheng Xiong, Yao Wang, Lei Wang, Yan Huang, Yang Xu and Yibing Guo, and data analyzed by Liancheng Xu, Jingjing Lu, Xiaohong Li and Mingyan Zhu. The manuscript was drafted and edited by Yicheng Xiong, Yao Wang, Mingyan Zhu and Haixin Qian.

Ethical approval and Patient Consent

Ethical approval was given by the medical ethics committee of Soochow University and written informed consent was obtained from every patient.

Competing Interests

The authors have declared that no competing interest exists.

References

1. Sirri E, Castro FA, Kieschke J, Jansen L, Emrich K, Gondos A, et al. Recent Trends in Survival of Patients With Pancreatic Cancer in Germany and the United States. Pancreas. 2016; 45: 908-14.
2. Xie CG, Wei SM, Chen JM, Xu XF, Cai JT, Chen QY, et al. Down-regulation of GEP100 causes increase in E-cadherin levels and inhibits pancreatic cancer cell invasion. PLoS One. 2012; 7: e37854.
3. Kallifatidis G, Rausch V, Baumann B, Apel A, Beckermann BM, Groth A, et al. Sulforaphane targets pancreatic tumour-initiating cells by NF-kappaB-induced antiapoptotic signalling. Gut. 2009; 58: 949-63.
4. Bao B, Ali S, Kong D, Sarkar SH, Wang Z, Banerjee S, et al. Anti-tumor activity of a novel compound-CDF is mediated by regulating miR-21, miR-200, and PTEN in pancreatic cancer. PLoS One. 2011; 6: e17850.
5. Li Y, Kong D, Ahmad A, Bao B, Sarkar FH. Pancreatic cancer stem cells: emerging target for designing novel therapy. Cancer Lett. 2013; 338: 94-100.
6. Shackleton M. Normal stem cells and cancer stem cells: similar and different. Semin Cancer Biol. 2010; 20: 85-92.
7. Chiou SH, Wang ML, Chou YT, Chen CJ, Hong CF, Hsieh WJ, et al. Coexpression of Oct4 and Nanog enhances malignancy in lung adenocarcinoma by inducing cancer stem cell-like properties and epithelial-mesenchymal transdifferentiation. Cancer Res. 2010; 70: 10433-44.
8. Wen J, Park JY, Park KH, Chung HW, Bang S, Park SW, et al. Oct4 and Nanog expression is associated with early stages of pancreatic carcinogenesis. Pancreas. 2010; 39: 622-6.
9. Zheng X, Carstens JL, Kim J, Scheible M, Kaye J, Sugimoto H, et al. Epithelial-to-mesenchymal transition is dispensable for metastasis but induces chemoresistance in pancreatic cancer. Nature. 2015; 527: 525-30.
10. Kurahara H, Takao S, Maemura K, Mataki Y, Kuwahata T, Maeda K, et al. Epithelial-mesenchymal transition and mesenchymal-epithelial transition via regulation of ZEB-1 and ZEB-2 expression in pancreatic cancer. J Surg Oncol. 2012; 105: 655-61.
11. Lamouille S, Xu J, Derynck R. Molecular mechanisms of epithelial-mesenchymal transition. Nat Rev Mol Cell Biol. 2014; 15: 178-96.
12. Batlle E, Clevers H. Cancer stem cells revisited. Nat Med. 2017; 23: 1124-34.
13. Scheel C, Weinberg RA. Cancer stem cells and epithelial-mesenchymal transition: concepts and molecular links. Semin Cancer Biol. 2012; 22: 396-403.
14. Kong D, Banerjee S, Ahmad A, Li Y, Wang Z, Sethi S, et al. Epithelial to mesenchymal transition is mechanistically linked with stem cell signatures in prostate cancer cells. PLoS One. 2010; 5: e12445.
15. Blick T, Hugo H, Widodo E, Waltham M, Pinto C, Mani SA, et al. Epithelial mesenchymal transition traits in human breast cancer cell lines parallel the CD44(hi)/CD24 (lo/-) stem cell phenotype in human breast cancer. J Mammary Gland Biol Neoplasia. 2010; 15: 235-52.
16. Peinado H, Portillo F, Cano A. Transcriptional regulation of cadherins during development and carcinogenesis. Int J Dev Biol. 2004; 48: 365-75.
17. Polyak K, Weinberg RA. Transitions between epithelial and mesenchymal states: acquisition of malignant and stem cell traits. Nat Rev Cancer. 2009; 9: 265-73.
18. Korpal M, Lee ES, Hu G, Kang Y. The miR-200 family inhibits epithelial-mesenchymal transition and cancer cell migration by direct targeting of E-cadherin transcriptional repressors ZEB1 and ZEB2. J Biol Chem. 2008; 283: 14910-4.
19. Li Y, VandenBoom TG, 2nd, Kong D, Wang Z, Ali S, Philip PA, et al. Up-regulation of miR-200 and let-7 by natural agents leads to the reversal of epithelial-to-mesenchymal transition in gemcitabine-resistant pancreatic cancer cells. Cancer Res. 2009; 69: 6704-12.
20. Zhang JP, Zeng C, Xu L, Gong J, Fang JH, Zhuang SM. MicroRNA-148a suppresses the epithelial-mesenchymal transition and metastasis of hepatoma cells by targeting Met/Snail signaling. Oncogene. 2014; 33: 4069-76.
21. Zhong K, Chen K, Han L, Li B. MicroRNA-30b/c inhibits non-small cell lung cancer cell proliferation by targeting Rab18. BMC Cancer. 2014; 14: 703.
22. Sugihara H, Ishimoto T, Watanabe M, Sawayama H, Iwatsuki M, Baba Y, et al. Identification of miR-30e* regulation of Bmi1 expression mediated by tumor-associated macrophages in gastrointestinal cancer. PLoS One. 2013; 8: e81839.
23. Cheng CW, Wang HW, Chang CW, Chu HW, Chen CY, Yu JC, et al. MicroRNA-30a inhibits cell migration and invasion by downregulating vimentin expression and is a potential prognostic marker in breast cancer. Breast Cancer Res Treat. 2012; 134: 1081-93.
24. Kao CJ, Martiniez A, Shi XB, Yang J, Evans CP, Dobi A, et al. miR-30 as a tumor suppressor connects EGF/Src signal to ERG and EMT. Oncogene. 2014; 33: 2495-503.
25. Zhong X, Li N, Liang S, Huang Q, Coukos G, Zhang L. Identification of microRNAs regulating reprogramming factor LIN28 in embryonic stem cells and cancer cells. J Biol Chem. 2010; 285: 41961-71.
26. Bao B, Ali S, Ahmad A, Li Y, Banerjee S, Kong D, et al. Differentially expressed miRNAs in cancer-stem-like cells: markers for tumor cell aggressiveness of pancreatic cancer. Stem Cells Dev. 2014; 23: 1947-58.
27. Mueller MT, Hermann PC, Witthauer J, Rubio-Viqueira B, Leicht SF, Huber S, et al. Combined targeted treatment to eliminate tumorigenic cancer stem cells in human pancreatic cancer. Gastroenterology. 2009; 137: 1102-13.
28. Shankar S, Nall D, Tang SN, Meeker D, Passarini J, Sharma J, et al. Resveratrol inhibits pancreatic cancer stem cell characteristics in human and KrasG12D

transgenic mice by inhibiting pluripotency maintaining factors and epithelial-mesenchymal transition. PLoS One. 2011; 6: e16530.

29. Ischenko I, Seeliger H, Kleespies A, Angele MK, Eichhorn ME, Jauch KW, et al. Pancreatic cancer stem cells: new understanding of tumorigenesis, clinical implications. Langenbecks Arch Surg. 2010; 395: 1-10.

30. Reya T, Morrison SJ, Clarke MF, Weissman IL. Stem cells, cancer, and cancer stem cells. Nature. 2001; 414: 105-11.

31. Garofalo M, Croce CM. Role of microRNAs in maintaining cancer stem cells. Adv Drug Deliv Rev. 2015; 81: 53-61.

32. Hao J, Zhang Y, Deng M, Ye R, Zhao S, Wang Y, et al. MicroRNA control of epithelial-mesenchymal transition in cancer stem cells. Int J Cancer. 2014; 135: 1019-27.

33. Bomken S, Fiser K, Heidenreich O, Vormoor J. Understanding the cancer stem cell. Br J Cancer. 2010; 103: 439-45.

34. Bhagwandin VJ, Bishop JM, Wright WE, Shay JW. The Metastatic Potential and Chemoresistance of Human Pancreatic Cancer Stem Cells. PLoS One. 2016; 11: e0148807.

35. Singh A, Settleman J. EMT, cancer stem cells and drug resistance: an emerging axis of evil in the war on cancer. Oncogene. 2010; 29: 4741-51.

36. Fan F, Samuel S, Evans KW, Lu J, Xia L, Zhou Y, et al. Overexpression of snail induces epithelial-mesenchymal transition and a cancer stem cell-like phenotype in human colorectal cancer cells. Cancer Med. 2012; 1: 5-16.

37. Wang H, Zhang G, Zhang H, Zhang F, Zhou B, Ning F, et al. Acquisition of epithelial-mesenchymal transition phenotype and cancer stem cell-like properties in cisplatin-resistant lung cancer cells through AKT/beta-catenin/Snail signaling pathway. Eur J Pharmacol. 2014; 723: 156-66.

38. Siemens H, Jackstadt R, Hunten S, Kaller M, Menssen A, Gotz U, et al. miR-34 and SNAIL form a double-negative feedback loop to regulate epithelial-mesenchymal transitions. Cell Cycle. 2011; 10: 4256-71.

39. Zuo QF, Cao LY, Yu T, Gong L, Wang LN, Zhao YL, et al. MicroRNA-22 inhibits tumor growth and metastasis in gastric cancer by directly targeting MMP14 and Snail. Cell Death Dis. 2015; 6: e2000.

40. Van der Auwera I, Limame R, van Dam P, Vermeulen PB, Dirix LY, Van Laere SJ. Integrated miRNA and mRNA expression profiling of the inflammatory breast cancer subtype. Br J Cancer. 2010; 103: 532-41.

41. Porkka KP, Pfeiffer MJ, Waltering KK, Vessella RL, Tammela TL, Visakorpi T. MicroRNA expression profiling in prostate cancer. Cancer Res. 2007; 67: 6130-5.

42. Yu H, Lin X, Wang F, Zhang B, Wang W, Shi H, et al. Proliferation inhibition and the underlying molecular mechanisms of microRNA-30d in renal carcinoma cells. Oncol Lett. 2014; 7: 799-804.

43. Bao B, Li Y, Ahmad A, Azmi AS, Bao G, Ali S, et al. Targeting CSC-related miRNAs for cancer therapy by natural agents. Curr Drug Targets. 2012; 13: 1858-68.

44. Zhong Z, Xia Y, Wang P, Liu B, Chen Y. Low expression of microRNA-30c promotes invasion by inducing epithelial mesenchymal transition in non-small cell lung cancer. Mol Med Rep. 2014; 10: 2575-9.

45. Ye Z, Zhao L, Li J, Chen W, Li X. miR-30d Blocked Transforming Growth Factor beta1-Induced Epithelial-Mesenchymal Transition by Targeting Snail in Ovarian Cancer Cells. Int J Gynecol Cancer. 2015; 25: 1574-81.